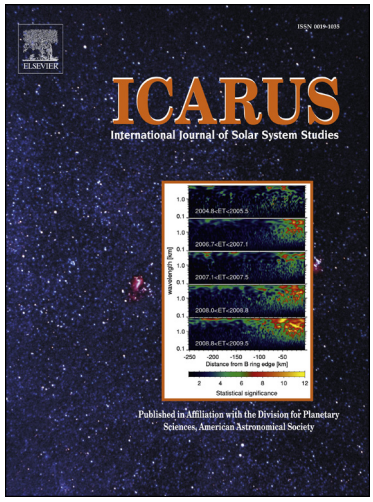

The Millimeter-Wavelength Sulfur Dioxide Absorption Spectra Measured Under Simulated Venus Conditions

Amadeo Bellotti, Paul G. Steffes

PII: S0019-1035(15)00129-3
DOI: http://dx.doi.org/10.1016/j.icarus.2015.03.028
Reference: YICAR 11510

To appear in: *Icarus*

Received Date: 9 December 2014
Revised Date: 24 March 2015
Accepted Date: 25 March 2015

Please cite this article as: Bellotti, A., Steffes, P.G., The Millimeter-Wavelength Sulfur Dioxide Absorption Spectra Measured Under Simulated Venus Conditions, *Icarus* (2015), doi: http://dx.doi.org/10.1016/j.icarus.2015.03.028

The Millimeter-Wavelength Sulfur Dioxide Absorption Spectra Measured Under Simulated Venus Conditions

Amadeo Bellotti
Paul G. Steffes

School of Electrical and Computer Engineering, Georgia Institute of Technology, Atlanta, GA 30332-0250

Abstract

Over 130 laboratory measurements of the 2-4 millimeter wavelength opacity of sulfur dioxide in a carbon dioxide atmosphere under simulated conditions for the upper Venus troposphere (temperatures between 308-343 K and pressures between 0.03- 2 bar) have been made. These measurements along with the centimeter wavelength measurements by Steffes et al. (2015) have been used to empirically assess existing formalisms for sulfur dioxide opacity in a carbon dioxide atmosphere (Fahd and Steffes (1992) and Suleiman et al. (1996)). The Van Vleck and Weisskopf Model (VVW) used by Fahd and Steffes with the JPL rotational line catalog (Pickett et al. (1998)) was found to fit 85.88% of all 500 measurements within the 2-sigma uncertainty. This work will improve the confidence in retrievals of the atmospheric abundance of sulfur dioxide from millimeter-wavelength observations of the Venus atmosphere.

Keywords: Venus, atmosphere, Radio observations, Atmospheres, composition, Spectroscopy

1. Introduction

Active and passive microwave remote sensing techniques have been extensively used in the study of our sister planet, Venus. Unlike Earth's atmosphere, the Venus atmosphere is mostly comprised of gaseous carbon dioxide (CO_2). CO_2 comprises 96.5% of the atmosphere along with gaseous nitrogen (N_2) at about 3.5% (Oyama et al., 1980). The Venus atmosphere has multiple trace constituents such as sulfur dioxide (SO_2), carbon monoxide (CO), water vapor (H_2O), carbonyl sulfide (OCS), and sufuric acid vapor (H_2SO_4) (Jenkins et al., 1994; Krasnopolsky and Pollack, 1994).

While the collision induced absorption of CO_2 dominates the continuum millimeter wave emission spectrum at Venus, spatial variations in the emission are attributable to cloud related gases such as SO_2, H_2SO_4 (g), and H_2SO_4 condensates (Steffes and Eshleman, 1981; Fahd and Steffes, 1992; Steffes, 1985). At higher pressures H_2SO_4 thermally dissociates, forming H_2O and SO_3, both of which exhibit relatively small amounts of microwave absorption at the abundance levels present in the Venus atmosphere (Ho et al., 1966; Steffes and Eshleman, 1981).

With the completion of the ESA Venus Express Mission, earth-based centimeter and millimeter-wavelength observations of Venus are becoming more important. The improved sensitivity of the NRAO EVLA (Extended Very Large Array) and the high resolution of ALMA (Atacama Large Millimeter Array) provide new capabilities for studying the atmosphere of Venus. Knowledge of the absorption properties of sulfur dioxide is important in the analysis of data from these earth-based observations.

Utilizing the millimeter-wavelength system at the Planetary Atmospheres

Laboratory at Georgia Institute of Technology, it has been possible to simulate the upper troposphere of Venus and take precision measurements of the millimeter-wavelength properties of sulfur dioxide. Using the measurements, a model that accurately predicts the opacity of sulfur dioxide in the Venus atmosphere has been verified. Applying this opacity model to a radiative transfer model will make it possible to determine the source of variations in the Venus millimeter-wavelength emission, such as were observed by de Pater et al. (1991) and Sagawa (2008).

Sagawa (2008) attributes the Venus millimeter-wavelength continuum brightness temperature variations to spatial variations in the abundances of both gaseous H_2SO_4 and SO_2 just below the cloud layer (48 km altitude). Sagawa (2008) has also suggested that the effects of both constituents can be distinguished based on differences in frequency dependencies of their millimeter-wavelength opacities. However, to accomplish this, high accuracy models must be developed that characterize the opacity of each constituent and their frequency dependence.

Observing how SO_2 varies spatially in the Venus atmosphere allows for a better understanding of the atmospheric dynamics that occur on Venus (Encrenaz et al., 2012, 2013; Sandor et al., 2010). Detailed thermochemical modeling indicates that the probable source of SO_2 in the lower atmosphere of Venus is due to volcanic activity, even though no volcanic activity has been directly observed (Esposito et al., 1988; Mahieux et al., 2014).

Radio observations of Venus in the 2-4 millimeter-wavelength range have the potential to allow for detection of variations in the abundance of SO_2 in the 35-70 km altitude range which includes the cloud layers. The altitude

range of the continuum emission in this wavelength range is constrained by the dominant opacity of CO_2. However localized variations in the emission can be attributed to localized abundance variations in cloud-related gases such as SO_2. Recently, observations of Venus with the Nobeyama millimeter-wave array of the 103 GHz continuum emission showed a 25% variation in brightness with position on the disk (Sagawa, 2008). While 1.3 and 2.0 cm continuum emissions from Venus indicated dark ($\sim$ 3%) polar regions consistent with increased H_2SO_4 vapor abundance due to vaporization of cloud condensate from the downwelling characteristic of Hadley cell circulation (Jenkins et al., 2002), the 3 mm maps show much stronger variations over a range of different locations, with some indication of diurnal variation. de Pater et al. (1991) reports significant variations (10%) in the 2.6 mm emission maps of Venus made with the Hat Creek Interferometer.

It is well understood that the microwave emission spectrum of Venus reflects the abundance and distribution of its constituents. A critical limiting factor in sensing these constituents is the knowledge of their microwave absorption properties under Venus conditions. The millimeter-wavelength absorption of SO_2 at 94.1 GHz has been measured by Fahd and Steffes (1992). Using newer technology it is possible to measure a wider spectrum with higher precision. Improved laboratory capabilities also allow a wider range of environmental conditions, similar to those actually being probed, to be simulated. The millimeter-wavelength system used in these experiments is able to reproduce conditions similar to those that exist on Venus. These results, in addition to centimeter-wave absorption spectra already measured by Steffes et al. (2015), have been used to help choose a model that best rep-

resents the centimeter- and millimeter-wavelength opacity of SO_2 in a CO_2 atmosphere.

2. Measurement Theory and System

Verifying the millimeter-wavelength absorption spectrum of SO_2 is important for the study of the atmosphere of Venus. Making measurements under simulated Venus conditions assures the accuracy of any model derived from such measurements.

In this experimental program, the quality factor (Q) of a resonant mode of a resonator is used to measure the absorption of a gas or gas mixture at that resonant frequency (Hanley and Steffes, 2007). The relationship between quality factor and absorption is given by

$$\alpha = 8.686\frac{\pi}{\lambda}\left(\frac{1-\sqrt{t_{loaded}}}{Q^m_{loaded}} - \frac{1-\sqrt{t_{matched}}}{Q^m_{matched}}\right) dB/km \qquad (1)$$

where α is the absorptivity of the gas, λ is the wavelength of the resonance (in km), t is the transmissivity of the resonance, and Q is the quality factor of the resonance. The subscripts *loaded* and *matched* refer the measurements made with the test gas and pure CO_2 respectively. The full derivation of this can be found in Appendix A.

Described below is the laboratory equipment and measurement procedure used in the measurement of the millimeter-wavelength absorptivity of gaseous SO_2 under simulated Venus conditions.

2.1. Millimeter-Wavelength Measurement System

The high-sensitivity millimeter-wavelength system used for measuring the opacity of gaseous sulfur dioxide under Venus conditions is similar to the one

used by Devaraj and Steffes (2011). The system is comprised of two subsystems for measuring different bands of the millimeter-wavelength spectrum (W-band/F-band). The simulator consists of a glass pressure chamber and a stable temperature chamber. Experiments using this system were done at pressures as high as 2 bars and temperatures up to 350 K. The W-band subsystem is used for measurements in the 2.7-4 millimeter-wavelength range while the F-band system is used for the 2-3 millimeter-wavelength range. Multiple resonances are measured in each band so as to develop an absorptivity spectrum. There are no resonances on the edge of the spectral range of each system; therefore no edge effects are present. The uncertainties associated with measurements using this system are described in Appendix B.

2.1.1. W-band Subsystem

The W-band measurement system is used to measure the 2.7-4 mm-wavelength properties of sulfur dioxide and shown in Figure 1.

A synthesized swept signal generator (HP 83650B) is used to generate a signal in the 12.5-18.3 GHz range which is fed to a times-six active multiplier chain (AMC) via low-loss, high frequency coaxial cables. The active multiplier then feeds the 75-110 GHz signals (swept over the range covered by each single resonance) to the Fabry-Perot resonator via WR-10 waveguides. The millimeter-wavelength radio frequency (RF) signal from the output port of the Fabry-Perot resonator (FPR) is fed via waveguide to a QuinStar Technology QMH series harmonic mixer. The local oscillator (LO) and the intermediate frequency (IF) are connected via an external diplexer. The harmonic mixer is locked to the 18th harmonic of the spectrum analyzer LO and is

used in the "external mixer" mode with the spectrum analyzer (HP 8564E).

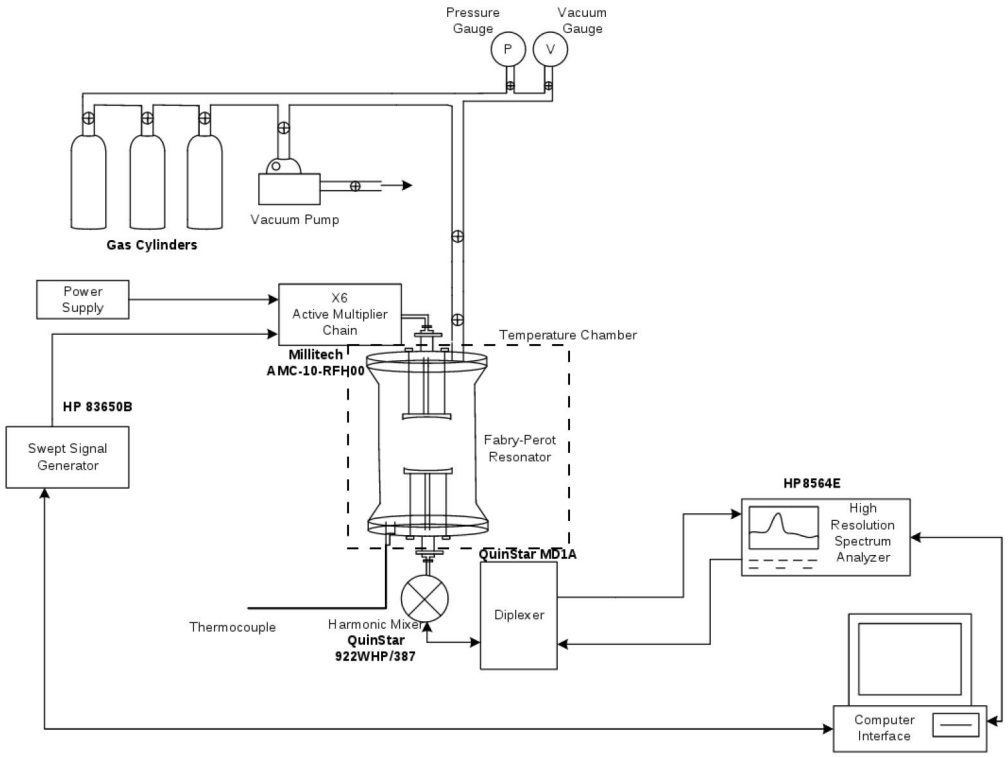

Figure 1: Block diagram of the W-band measurement system. Solid lines represent the electrical connections and the arrows show the direction of the signal propagation. Valves controlling the flow of gasses are shown by small crossed circles.

2.1.2. F-band Subsystem

The F-band measurement system is used to measure the 2-3 mm-wavelength properties of sulfur dioxide and is shown in Figure 2.

The swept signal generator (HP 83650B) is used to generate a signal in the 33-50 GHz range which is amplified and fed through a frequency tripler. The output of the tripler is fed to the input of the FPR via WR-8 waveguides.

The RF signal from the output port of the FPR is fed to a harmonic mixer which can operate with an LO frequency as high as 18 GHz. An external diplexer is used to combine the IF and LO signals. For a particular RF and IF frequency, the LO frequency can be computed using

$$f_{LO} = \frac{f_{RF} - f_{IF}}{N_H} \tag{2}$$

where N_H is the lowest integer such that $f_{LO} < 18GHz$.

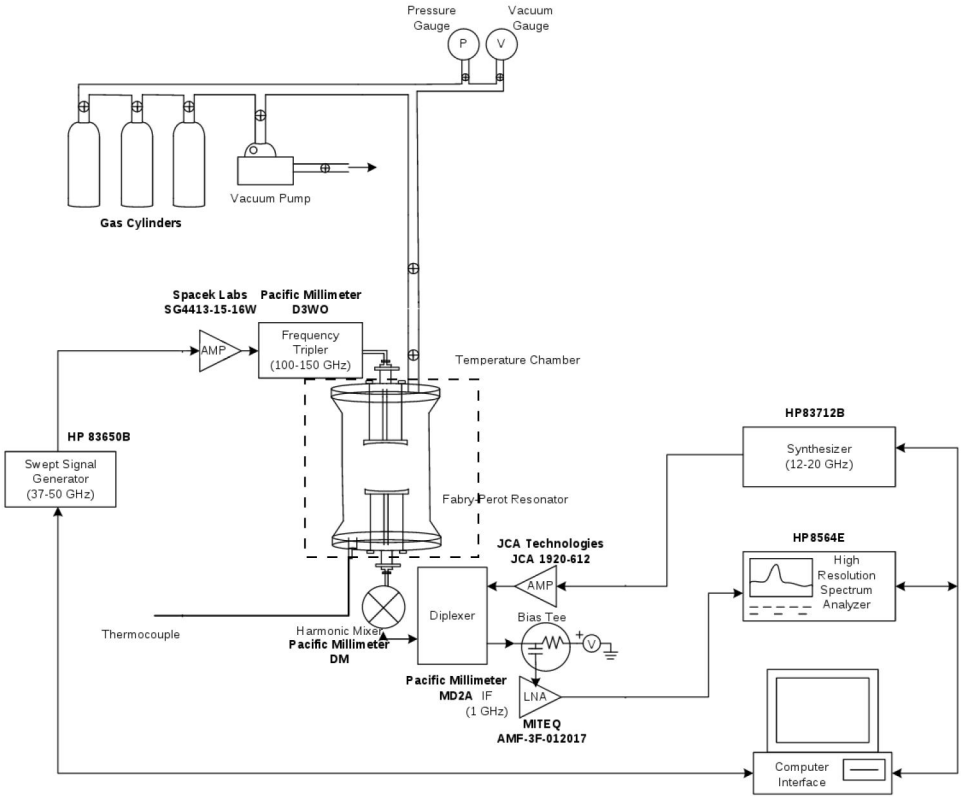

Figure 2: Block diagram of the F-band measurement system. Solid lines represent the electrical connections and the arrows show the direction of the signal propagation. Valves controlling the flow of gasses are shown by small crossed circles.

2.1.3. Data Handling Subsystem

The data acquisition system consists of a computer connected to the spectrum analyzer (HP 8564E), swept signal generator (HP 83650B), and continuous wave (CW) signal generator (HP 83712B, the local oscillator for the F-Band system) via a general purpose interface bus (GPIB). The instruments are controlled via Matlab script and their appropriate programming language. The software used is similar to that described in Devaraj and Steffes (2011) with modifications for equipment changes.

2.2. Measurement Procedure

The most important prerequisite for performing measurement of gas properties is ensuring a leak-proof system. Pressure integrity was verified using two methods: the first is by drawing a vacuum inside the FPR and verifying the integrity of the vacuum over time. The second is by adding a positive pressure of CO_2 to the system and making sure there are no leaks in any of the connectors and valves. Ensuring a leak-proof system allows for not only precise measurements but also ensures no toxic gases are released into the testing environment.

After the system is ensured to be leak-proof and at a stable temperature, a vacuum is drawn and a measurement is taken using the appropriate subsystem (W-band for 2.7-4 mm-wavelengths, F-band for 2-3 mm-wavelengths). This allows for a baseline measurement of the FPR's resonances and the quality factor. Once this baseline is established the gas under test is added to the system.

Once the gas temperature has stabilized, another set of tests measuring the resonant frequencies along with the quality factors is taken. More gas is

added and the procedure is repeated until measurements at all suitable pressures are taken. A vacuum is drawn once again but this time it is pumped overnight due to the possibility of adsorption (or "sticking") of the gas being tested (SO_2) to metal surfaces inside the vessel. This second vacuum measurement is taken to measure any possible system drift.

Once the second vacuum measurement is taken, CO_2 is then added to the chamber until the resonances are matched to the same frequency as the test gas (note that at the pressures and frequencies used for our experiment, pure CO_2 is essentially lossless). Again measurements are taken and this is repeated for every pressure of the test gas. Once completed a vacuum is again drawn and another test is taken.

Lastly the system is set up for a transmissivity test where we measure t (equation A.5) for each given resonant frequency. This is done by bypassing the Fabry-Perot resonator and connecting the input and output waveguides through a WR-10 20 dB directional coupler. The signal level is then measured and used to calculate the transmissivity, t. The system is then set back up and is ready for a new test.

3. Results

High accuracy laboratory measurements of the temperature and pressure dependence of the millimeter-wavelength absorption of gaseous SO_2 in a CO_2 atmosphere have been conducted at 308 K and 345 K and at pressures from 30 mbar to 3 bars for wavelengths between 2-4 millimeters (Table 1). Figures 3–8 show the typical results of these absorptivity measurements with the accompanying 2σ uncertainties. For comparison purposes, these plots

also show two known formalisms of SO_2's absorptivity. One developed by Suleiman et al. (1996) and the second by Fahd and Steffes (1992) but using the new JPL line catalog (Pickett et al., 1998).

The Suleiman et al. (1996) model employs a Ben-Reuven lineshape which is the quantum mechanical equation which treats collisional broadening as collisions on a classical oscillator. The formalism employs pressure-broadened line widths, coupling elements, and pressure shift terms (Waters, 1976). The Fahd and Steffes (1992) formalism uses a traditional Van Vleck-Weisskopf lineshape which assumes that the collision-induced phase shifts and momentum-reversing collisions are random (Waters, 1976) and thus no coupling elements or presure-shift terms are required.

Since each resonance has a different quality factor (Q), each spectral data point will have a different uncertainty. A low transmissivity, t, for a specific resonance will result in a low signal to noise ratio, which in turn affects the sensitivity of each resonance. The test gas can become opaque enough such that the resonance is no longer detectable. When this happens the resonance is not plotted or used in the model analysis.

Table 1: Testing matrix for SO_2's microwave absorption properties at 2-4 millimeter-wavelength.

Temperature	SO_2 Pressure	CO_2 Pressure	Subsystem
308 K	110 mbar	0, 0.83, 1.87 bar	W-band
343 K	85 mbar	0, 0.84, 1.92 bar	W-band
343 K	51 mbar	0, 0.87, 1.94 bar	W-band
343 K	76 mbar	0, 0.83, 1.87 bar	F-band
343 K	28 mbar	0, 0.91, 1.97 bar	F-band
308 K	25 mbar	0, 0.97, 2.00 bar	F-band

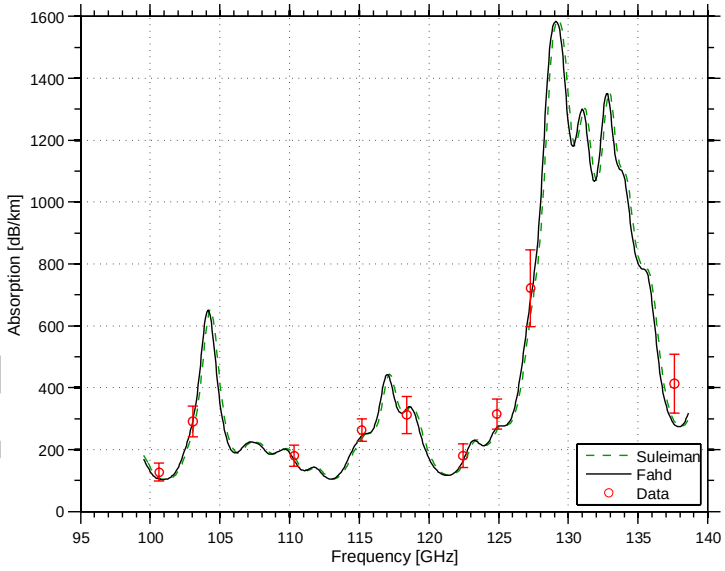

Figure 3: Opacity data using the 2-3 mm-wavelength system for a mixture of 76 mbars of SO_2 and 14 mbars of N_2 at a temperature of 344.4 K compared to various models

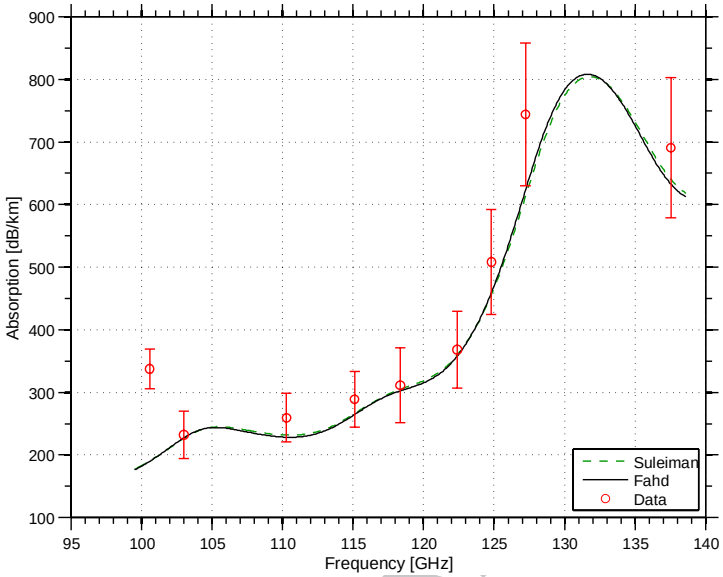

Figure 4: Opacity data using the 2-3 mm-wavelength system for a mixture of 76 mbars of SO_2 and 833 mbars of CO_2 at a temperature of 344.6 K compared to various models

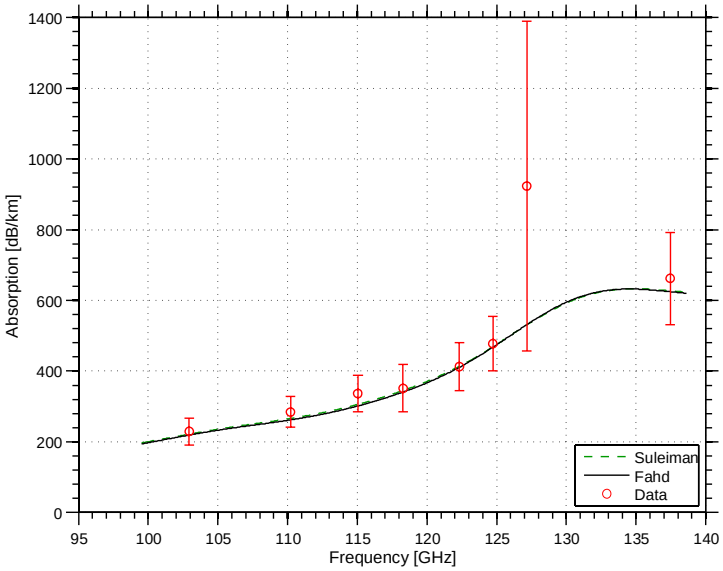

Figure 5: Opacity data using the 2-3 mm-wavelength system for a mixture of 76 mbars of SO_2 and 1.877 bars of CO_2 at a temperature of 343.9 K compared to various models

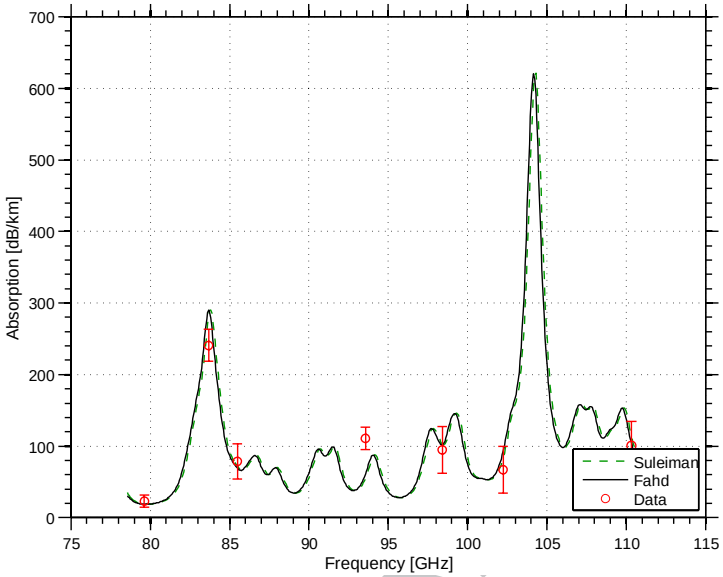

Figure 6: Opacity data using the 2.7-4 mm-wavelength system for a mixture of 51 SO_2 and 9 mbars of N_2 at a temperature of 343.1 K compared to various models

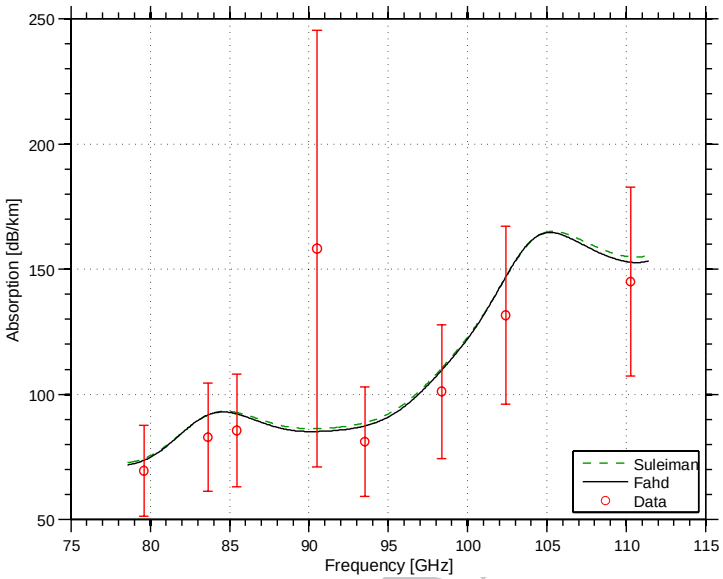

Figure 7: Opacity data using the 2.7-4 mm-wavelength system for a mixture of 51 mbars of SO_2 and 867 mbars of CO_2 at a temperature of 343.6 K compared to various models

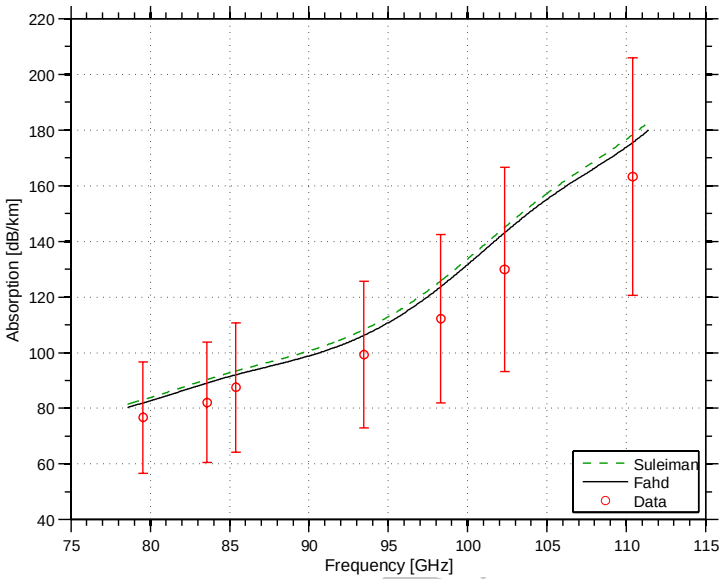

Figure 8: Opacity data using the 2.7-4 mm-wavelength system for a mixture of 51 mbars of SO_2 and 1.953 bars of CO_2 at a temperature of 343.6 K compared to various models

3.1. Suggested Model

Results indicate that the models for the millimeter-wavelength opacity from SO_2 in a CO_2 atmosphere by Suleiman et al. (1996) and Fahd and Steffes (1992) are both valid over the entire millimeter-wavelength range under simulated conditions for the upper atmosphere of Venus. Previous *centimeter-wavelength* laboratory measurements of SO_2 in a CO_2 atmosphere were conducted by Steffes et al. (2015). Based on their data and the data presented in this work, the suggested model is that from Fahd and Steffes (1992), but using the updated SO_2 line catalog from Pickett et al. (1998). This model employs the Van Vleck-Weisskopf lineshape, and was developed from measurements of SO_2/CO_2 mixtures conducted at room temperature. As per Fahd and Steffes (1992), we employ only the rotational line catalog to

compute opacity (JPL spectral line catalog, (Pickett et al., 1998)). Table 2 shows how both models perform relative to the centimeter- and millimeter-wavelength laboratory data. Since most of the SO_2 absorption lines are at millimeter-wavelengths, the millimeter-wavelength data fits the models better.

When applied to a disk-averaged radiative transfer model similar to that of Fahd and Steffes (1992), the difference in predicted emission using the two models differs by 1.2 K at 8.7 GHz to 0.1 K at 100 GHz. While the resulting difference is very small, this work has verified the accuracy of the frequency dependence in the two models for SO_2 opacity. The only previous laboratory measurement (Fahd and Steffes, 1992) measured the millimeter-wavelength absorption of SO_2 at only a single wavelength (3.2 mm).

Table 2: The percentage of the measured data points within 2σ uncertainty of the different models

SO_2 opacity model	Centimeter Wavelength (1.5-8 GHz) Steffes et al. (2015)	Millimeter Wavelength (80-150 GHz)	Total
Fahd and Steffes (1992)	82.97%	92.86%	85.88%
Suleiman (1997)	62.98%	88.10%	70.37%

4. Conclusion

The objective of this work has been to advance the understanding of the millimeter-wavelength properties of gaseous sulfur dioxide under Venus

conditions. Extensive laboratory measurements of the 2-4 mm-wavelength properties of sulfur dioxide under simulated upper troposphere conditions of Venus were conducted. These measurements along with previous laboratory measurements (Fahd and Steffes, 1992; Suleiman et al., 1996; Steffes et al., 2015) have been used to validate absorption formalisms across all microwave frequencies.

The formalism for sulfur dioxide opacity developed by Fahd and Steffes (1992) using the updated line catalog from Pickett et al. (1998) is able to fit 85.88% of the laboratory data (centimeter-wavelength done by Steffes et al. (2015), millimeter-wavelength presented in this work) within 2σ uncertainty. The bounds verified by this laboratory data are frequencies between 1-150 GHz, temperatures between 307-550 K, and concentrations between 0-100% SO_2/volume.

As a next step we are planning modifications to our laboratory system which will allow for measurement of the 2–4 millimeter-wavelength absorption spectrum of gaseous H_2SO_4 under simulated Venus conditions.

Acknowledgement

This work was supported by the NASA Planetary Atmospheres Program under Grant NNX11AD66G. We especially thanks Ms. Siri Anne Gomes and Dr. Doug King of Airgas USA for assistance in verifying gas mixture compositions.

Appendix A. Measurement Theory

The quality factor of a resonance is given by (Mattaei and Jones, 1980)

$$Q = \frac{2\pi f_0 \text{ x Energy Stored}}{\text{Average Power Loss}} \tag{A.1}$$

where f_0 is the resonant frequency. The Q of a resonance can be measured directly from f_0 by dividing it by its half-power bandwidth (HPBW).

$$Q = \frac{f_0}{HPBW} \tag{A.2}$$

The Q of a lossy gas (ϵ'/ϵ'') and its opacity are related by

$$\alpha \approx \frac{\epsilon''\pi}{\epsilon'\lambda} = \frac{1}{Q_{gas}}\frac{\pi}{\lambda} \tag{A.3}$$

where ϵ' and ϵ'' are the real and imaginary permittivity of the gas, λ is the wavelength in km, and α is the absoptivity of the gas in Nepers/km (1 Neper = 8.686 dB) (DeBoer and Steffes, 1994). Since Q is affected by more than just the gas under test, the Q of the gas-filled resonator is given by

$$\frac{1}{Q^m_{loaded}} = \frac{1}{Q_{gas}} + \frac{1}{Q_r} + \frac{1}{Q_{ext1}} + \frac{1}{Q_{ext2}} \tag{A.4}$$

where Q^m_{loaded} is the measured quality factor of a resonance in the presence of a test gas, Q_{gas} is the quality factor of the gas under test, Q_r is the quality factor of the evacuated resonator in the absence of coupling losses, and Q_{ext1} and Q_{ext2} are the external coupling losses. Since the resonator used is symmetric, we assume $Q_{ext1} = Q_{ext2}$. Coupling losses can be derived from the transmissivity $t = 10^{-S/10}$, where S is the measured insertion loss of the resonator in decibels (dB) at the frequency of a particular resonance using the following relationship (Mattaei and Jones, 1980)

$$t = \left[2\frac{Q^m}{Q_{ext}}\right]^2, \tag{A.5}$$

$$Q_{ext} = \frac{2Q^m}{\sqrt{t}} \tag{A.6}$$

Q_r is related to the measured Q at a vacuum by

$$\frac{1}{Q^m_{vac}} = \frac{1}{Q_r} + \frac{1}{Q_{ext1}} + \frac{1}{Q_{ext2}} \tag{A.7}$$

where Q^m_{vac} is the measured Q under vacuum conditions. Substituting equation (A.6) into equations (A.4) and (A.7) gives

$$\frac{1}{Q_{gas}} = \frac{1-\sqrt{t_{loaded}}}{Q^m_{loaded}} - \frac{1-\sqrt{t_{vac}}}{Q^m_{vac}} \tag{A.8}$$

where t_{loaded} and t_{vac} are the transmissivity of the resonance taken in loaded and vacuum conditions respectively. When gas is added to the resonator there is a shift in the center frequency corresponding to the refractive index of the test gas. Since the quality factor is reliant on the center frequency this will affect the comparison between the two measurements, even if the gas being tested is lossless. This effect is called dielectric loading (DeBoer and Steffes, 1994). This effect can be corrected by performing additional measurements of the quality factor with a lossless gas present. Adding the lossless gas shifts the center frequency of the resonances, and by adding more or less gas the center frequency can be adjusted to be exactly the same as the lossy gas. These measurements are used in place of the vacuum measurements in equation (A.8) and by converting Nepers/km to dB/km equation (A.3) bccomcs

$$\alpha = 8.686\frac{\pi}{\lambda}\left(\frac{1-\sqrt{t_{loaded}}}{Q^m_{loaded}} - \frac{1-\sqrt{t_{matched}}}{Q^m_{matched}}\right) dB/km \tag{A.9}$$

An important note is that an absorption coefficient of 1 Nepers/km = 2 optical depths per km (or km^{-1}) = 8.686 dB/km. The first notation is used in electrical engineering, the second is the usual form in physics and astronomy, and the third is the common (logarithmic) form. The third form is often used in order to avoid a possible factor-of-two ambiguity.

It is also important to know the refractive index n_{ri} of the gas under test since small changes in this value could alter the way electromagnetic waves propagate through the medium. The refractive index of a gas is measured by the frequency shift exhibited by the resonances and can be used to determine the refractive index to a high level of accuracy. The refractivity (N) of a gas is given by

$$N = 10^6(n_{ri} - 1) \tag{A.10}$$

The refractivity is measured by comparing the center frequency of the resonator under gaseous conditions to the peak frequency of the resonances at a vacuum and is give by

$$N = \frac{10^6(f_{vac} - f_{gas})}{f_{gas}} \tag{A.11}$$

where N is the refractivity of the entire gas mixture f_{gas} is the peak frequency of the resonance in presence of the test gas and f_{vac} the peak frequency of the resonance at a vacuum (Tyler and Howard, 1969). The overall refractivity of the mixture is the sum of the refractivity of the individual gases scaled with their respective mole fractions.

Appendix B. Measurement Uncertainties

There are five sources of uncertainty for absorptivity measurements using this system (Hanley and Steffes, 2007): instrumentation errors and electrical

noise (Err_{inst}), errors in dielectric matching (Err_{diel}), errors in transmissivity measurement (Err_{trans}), errors due to resonance asymmetry (Err_{asym}), and errors in measurement conditions (Err_{cond}) resulting from uncertainties in temperature, pressure, and mixing ratio. The term Err represents 2σ uncertainties.

Instrumental errors and electrical noise are due to the limited sensitivity of the electrical devices and their ability to accurately measure bandwidth ($BW_{measured}$) and the center frequency (f_o). Electrical noise arises from the limited-stability frequency references and the noise of the internal electronics. Electrical noise is uncorrelated and the best estimate of instrumental uncertainty is the statistical variance of multiple measurements. The contribution of electrical noise is outlined in Hanley et al. (2009),

$$Err_n = B \times \frac{S_n}{\sqrt{n_{samples}}} \tag{B.1}$$

where S_n is the sample standard deviation, B is the confidence coefficient and $n_{samples}$ is the number of independent measurements. For the millimeter-wavelength system, five sets of independent measurements of each resonance are taken. A confidence coefficient (B) of 2.776 is used (for each 5 sample data point). This corresponds to the 95% confidence interval (approximately 2σ) (Student, 1908). The center frequency standard deviation is very small and its effect on the uncertainty in Q is negligible. Therefore, S_n is the standard deviation of the bandwidth of the measurements.

The HP 8564E spectrum analyzer is used for measuring the resonances in the millimeter-wavelength system. Its manufacturer-specified instrumental uncertainties are 3σ values (Hewlett-Packard, 1997). The 3σ standard deviation for the center frequency and bandwidth are estimated by

$$Err_o \leq \pm(f_o \times f_{ref\,acc} + 0.05 \times SPAN + 0.15 \times RBW + 10)(Hz) \quad \text{(B.2)}$$

$$Err_{BW} \leq \pm(BW_{measured} \times f_{ref\,acc} + 4 \times N_H + 2 \times LSD)(Hz) \quad \text{(B.3)}$$

where $f_{ref\,acc}$ is given as

$$f_{ref\,acc} = (aging \times time\ since\ calibration) + inital\ achievable\ accuracy + temperature\ stability \quad \text{(B.4)}$$

and f_o, SPAN, RBW, N_H, and LSD are the center frequency, frequency span, resolution bandwidth, harmonic number, and least significant digit of the bandwidth measurement, respectively. LSD is calculated as

$$LSD = 10^x \quad \text{(B.5)}$$

where x is the the smallest positive integer value of x such that SPAN $< 10^{x+4}$. For SPAN $\leq$ 2 MHz$\times N_h$, Equation (B.2) becomes

$$Err_o \leq \pm(f_o \times f_{ref\,acc} + 0.01 \times SPAN + 0.15 \times RBW + 10)(Hz) \quad \text{(B.6)}$$

For the spectrum analyzer used, $f_{ref\,acc}$ reduces to

$$f_{ref\,acc} = (10^{-7} \times years\ since\ calibrated) + 3.2 \times 10^{-8} \quad \text{(B.7)}$$

The worst case scenario is used to transform the uncertainty in center frequency and bandwidth for both loaded and dielectrically matched measurements into an uncertainty in absorptivity as described in DeBoer and Steffes (1994).

$$Err_{\Psi}^2 = \langle F_l^2 \rangle + \langle F_m^2 \rangle - \langle F_l F_m \rangle \tag{B.8}$$

where

$$\langle F_i^2 \rangle = \frac{\Upsilon_i^2}{f_{oi}^2}\left[\frac{Err_o^2}{Q_l^2} + Err_{BW}^2 + Err_{Ni}^2 + \frac{2Err_o Err_{BW}}{Q_i}\right], i = l, m \tag{B.9}$$

$$\langle F_l F_m \rangle = -\frac{\Upsilon_l \Upsilon_m}{f_{ol} f_{om}}\left[\frac{Err_o^2}{Q_i Q_m} + Err_{BW}^2 + \frac{Err_o Err_{BW}}{Q_l} + \frac{Err_o Err_{BW}}{Q_m}\right] \tag{B.10}$$

$$Q_i = \frac{f_{oi}}{f_{BWi}}, i = l, m \tag{B.11}$$

$$\Upsilon_i = 1 - \sqrt{t}, i = l, m \tag{B.12}$$

where l, m denote loaded and dielectrically matched cases respectively and $f_{ol,om}$ and $f_{BWl,BWm}$ represent center frequency and bandwidth of loaded and dielectrically matched cases respectively. The 2σ uncertainty of the measured gas absorption due to instrumental errors and electrical noise is given by

$$Err_{inst} = \pm\frac{8.686\pi}{\lambda} Err_{\Psi}\ (dB/km) \tag{B.13}$$

where λ is the wavelength in km.

Errors in dielectric matching occur when the center frequency of the matched measurements are not precisely aligned with the center frequency of the loaded measurement. Since the Q of the resonator can vary slightly, this causes an uncertainty in the Q of the matched measurement at the true center frequency of the loaded measurement. The method used to calculate the magnitude of this effect is similar to Hanley and Steffes (2007). While this error is the smallest due to the high precision of the software controlled matching, it is important to calculate and account for. The magnitude of this

effect is calculated by comparing the Q of the three vacuum measurements to that of the dielectric matched measurements

$$\left(\frac{dQ}{df}\right)_i = \left|\frac{Q_{vac,i} - Q_{matched,i}}{f_{vac,i} - f_{matched,i}}\right| \text{ for } i = 1, 2, 3 \tag{B.14}$$

The maximum of the three values is used to calculate a dQ value

$$dQ = \left(\frac{dQ}{df}\right)_{max} \times |f_{loaded} - f_{matched}| \tag{B.15}$$

where f_{loaded} and $f_{matched}$ are the center frequencies of the resonances under loaded and matched conditions. The error in absorptivity due to imperfect dielectric matching is then computed by propagating $\pm dQ$ through Equation (A.9).

$$Err_{diel} = \frac{8.686\pi}{\lambda} \times \left|\left(\frac{1-\sqrt{t_{loaded}}}{Q^m_{loaded}} - \frac{1-\sqrt{t_{matched}}}{Q^m_{matched}+dQ}\right) - \left(\frac{1-\sqrt{t_{loaded}}}{Q^m_{loaded}} - \frac{1-\sqrt{t_{matched}}}{Q^m_{matched}-dQ}\right)\right| \quad (dB/km) \tag{B.16}$$

Transmissivity errors are due to the uncertainties in the measurement amplitude. This is caused by variations in gains of losses of the millimeter-wavelength instruments (signal generators and spectrum analyzer), cables, adapters, and waveguides used in this system. This is done by taking multiple test measurements of signal loss through the system without the FPR and finding the standard deviation (S_N) of the signal loss and weighing it by its confidence coefficient

$$Err_{msl} = \frac{4.303}{\sqrt{3}} S_N \tag{B.17}$$

For the millimeter-wavelength system, the signal level measurements involve sampling the RF power with a WR-10 20 dB directional coupler to feed the harmonic mixer for down-conversion and detection. While this ensures that the input to the harmonic mixer does not exceed its maximum allowed input power of -10 dBm, the WR-10 20dB directional coupler does not uniformly sample the input signal throughout the entire frequency range. To compensate for this, an additional 1.5 dB uncertainty is added to insertion loss error. The signal generator has a temperature stability of 1 dB/10° C, but an internal temperature equilibrium is reached after two hours (Hewlett-Packard, 1997). Since the instruments are operated at a constant temperature this uncertainty can be disregarded. The total uncertainty in insertion loss for the millimeter-wavelength system is calculated by

$$Err_{ins\,loss} = Err_{msl} + 1.5\ (dB) \tag{B.18}$$

The error in insertion loss is used to compute the transmissivity error

$$Err_{t,i} = \frac{1}{2}(10^{-S_i - Err_{ins\,loss}} - 10^{-S_i + Err_{ins\,loss}}), i = l, m \tag{B.19}$$

where l, m are the loaded and matched cases, respectively, and S is the insertion loss of the resonator. This is used to compute the 2σ uncertainties in opacity and is expressed as

$$Err_{trans} = \frac{8.686\pi}{2\lambda} \times \left| \left(\frac{\sqrt{t_l + Err_{t,l}} - \sqrt{t_l - Err_{t,l}}}{Q^m_{loaded}} - \frac{\sqrt{t_m - Err_{t,m}} - \sqrt{t_m + Err_{t,m}}}{Q^m_{matched}} \right) \right| (dB/km). \tag{B.20}$$

Errors from asymmetry are due to the asymmetric nature of the resonances. These are more prominent at low temperatures and short wavelengths. Errors due to the asymmetry result from the disproportionate asymmetric broadening of the loaded measurements compared to the matched measurements. Equivalent full bandwidths based on assuming symmetry of the high and low sides of the resonances are calculated as

$$BW_{high} = 2 \times (f_{high} - f_{center}) \tag{B.21}$$

$$BW_{low} = 2 \times (f_{center} - f_{low}) \tag{B.22}$$

where $BW_{high}, BW_{low}, f_{high}, f_{center}$, and f_{low} are the high bandwidth, low bandwidth, higher frequency half power point, center frequency, and lower frequency half power point, respectively. For a perfectly symmetric resonance, $BW_{high} = BW_{low}$. The difference between the opacities calculated using BW_{high} and BW_{low} is defined as Err_{asym} and is calculated by

$$Err_{asym} = \frac{8.686\pi}{\lambda} \times \left| \left(\frac{1-\sqrt{t_{loaded}}}{Q^m_{loaded,high}} - \frac{1-\sqrt{t_{matched}}}{Q^m_{matched,high}} \right) - \left(\frac{1-\sqrt{t_{loaded}}}{Q^m_{loaded,low}} - \frac{1-\sqrt{t_{matched}}}{Q^m_{matched,low}} \right) \right| \quad (dB/km) \tag{B.23}$$

where $Q^m_{matched,high/low}$ and $Q^m_{loaded,high/low}$ are the measured Q's evaluated using the high and low bandwidths for loaded and matched cases.

The uncertainties in measured temperature, pressure, and concentration in the millimeter-wavelength system contribute to the total uncertainty due to the measurement conditions (Err_{cond}). While uncertainties in mea-

surement conditions do not directly affect the measurements of millimeter-wavelength absorptivity, they still need to be accounted for when evaluating the opacity formalisms. It is computed by

$$Err_{cond} = \sqrt{Err_{temp}^2 + Err_p^2 + Err_c^2}\ (dB/km) \tag{B.24}$$

with Err_{temp}, Err_p, and Err_c representing the 2σ uncertainties in temperature, pressure, and concentration (or mole fraction) respectively. Each of these are calculated by taking the maximum modeled opacity with each uncertainty minus the minimum modeled opacity and halving the difference.

Since Err_{cond} is dependent on the opacity model, this uncertainty is maintained separately from Err_{tot}. Thus the total 95% confidence for the measurement uncertainty is expressed in dB/km as per Hanley and Steffes (2007)

$$Err_{tot} = \sqrt{Err_n^2 + Err_{diel}^2 + Err_{trans}^2 + Err_{asym}^2}\ (dB/km). \tag{B.25}$$

Accuracy of Constituents

It is necessary to ensure that the gases used in each experiment are correctly characterized. The CO_2 used was Ultra High Purity (UHP) grade. The test gas was comprised of 84.7% SO_2 and 15.3% N_2. In our experiments, the partial pressure of N_2 never exceeds 20 mbar. While including N_2 allows for a simulation similar to that of the Venus atmosphere, it does not affect the outcome of our models.

References

de Pater, I., Schloerb, F., Rudolph, A., 1991. Venus imaged with the hat creek interferometer in the j = 1 0 {CO} line. Icarus 90 (2), 282 – 298. URL http://www.sciencedirect.com/science/article/pii/0019103591901075

DeBoer, D. R., Steffes, P. G., 1994. Laboratory measurements of the microwave properties of H2S under simulated jovian conditions with an application to neptune. Icarus 109 (2), 352 – 366. URL http://www.sciencedirect.com/science/article/pii/S0019103584710992

Devaraj, K., Steffes, P. G., 2011. The Georgia Tech millimeter-wavelength measurement system and some applications to the study of planetary atmospheres. Radio Science 46 (2), 149–157. URL http://dx.doi.org/10.1029/2010RS004433

Encrenaz, T., Greathouse, T. K., Richter, M. J., Lacy, J., Widemann, T., Bzard, B., Fouchet, T., deWitt, C., Atreya, S. K., 2013. Hdo and so2 thermal mapping on venus. A&A 559, A65. URL http://dx.doi.org/10.1051/0004-6361/201322264

Encrenaz, T., Greathouse, T. K., Roe, H., Richter, M., Lacy, J., Bzard, B., Fouchet, T., Widemann, T., 2012. Hdo and so2 thermal mapping on venus: evidence for strong so2 variability. A&A 543, A153. URL http://dx.doi.org/10.1051/0004-6361/201219419

Esposito, L. W., Copley, M., Eckert, R., Gates, L., Stewart, A. I. F., Worden, H., 1988. Sulfur dioxide at the venus cloud tops, 19781986. Journal of

Geophysical Research: Atmospheres 93 (D5), 5267–5276.
URL http://dx.doi.org/10.1029/JD093iD05p05267

Fahd, A. K., Steffes, P. G., 1992. Laboratory measurements of the microwave and millimeter-wave opacity of gaseous sulfur dioxide (SO_2) under simulated conditions for the Venus atmosphere. Icarus 97 (2), 200–210.
URL http://dx.doi.org/10.1016/0019-1035(92)90128-T

Hanley, T. R., Steffes, P. G., 2007. A high-sensitivity laboratory system for measuring the microwave properties of gases under simulated conditions for planetary atmospheres. Radio Science 42 (6).
URL http://dx.doi.org/10.1029/2007RS003693

Hanley, T. R., Steffes, P. G., Karpowicz, B. M., 2009. A new model of the hydrogen and helium-broadened microwave opacity of ammonia based on extensive laboratory measurements. Icarus 202 (1), 316 – 335.
URL http://www.sciencedirect.com/science/article/pii/S0019103509000451

Hewlett-Packard, 1997. HP 8560 E-Series Spectrum Analyzer Calibration Guide. Hewlett-Packard, Santa Rosa, CA.

Ho, W., Kaufman, I. A., Thaddeus, P., 1966. Laboratory measurement of microwave absorption in models of the atmosphere of venus. Journal of Geophysical Research 71 (21), 5091–5108.
URL http://dx.doi.org/10.1029/JZ071i021p05091

Jenkins, J. M., Kolodner, M. A., Butler, B. J., Suleiman, S. H., Steffes, P. G., 2002. Microwave remote sensing of the temperature and distribution of sul-

fur compounds in the lower atmosphere of venus. Icarus 158 (2), 312 – 328.
URL http://www.sciencedirect.com/science/article/pii/S0019103502968946

Jenkins, J. M., Steffes, P. G., Hinson, D. P., Twicken, J. D., Tyler, G., 1994. Radio occultation studies of the venus atmosphere with the magellan spacecraft: 2. results from the october 1991 experiments. Icarus 110 (1), 79 – 94.
URL http://www.sciencedirect.com/science/article/pii/S0019103584711080

Krasnopolsky, V., Pollack, J., 1994. H2o-h2so4 system in venus' clouds and ocs, co, and {H2SO4} profiles in venus' troposphere. Icarus 109 (1), 58 – 78.
URL http://www.sciencedirect.com/science/article/pii/S0019103584710773

Mahieux, A., Vandaele, A., Robert, S., Wilquet, V., Drummond, R., Chamberlain, S., Belyaev, D., Bertaux, J., 2014. Venus mesospheric sulfur dioxide measurement retrieved from {SOIR} on board venus express. Planetary and Space Science (0), –.
URL http://www.sciencedirect.com/science/article/pii/S0032063314004036

Mattaei, G. L., Jones, E., 1980. Microwave filters, impedance matching networks and coupling structures. McGraw-Hill, New York.

Oyama, V. I., Carle, G. C., Woeller, F., Pollack, J. B., Reynolds, R. T., Craig, R. A., 1980. Pioneer venus gas chromatography of the lower atmosphere of venus. Journal of Geophysical Research: Space Physics 85 (A13), 7891–7902.
URL http://dx.doi.org/10.1029/JA085iA13p07891

Pickett, H., Poynter, R., Cohen, E., Delitsky, M., Pearson, J., Muller, H., 1998. Submillimeter, millimeter, and microwave spectral line catalog. Journal of Quantitative Spectroscopy and Radiative Transfer 60 (5), 883 – 890.
URL http://www.sciencedirect.com/science/article/pii/S0022407398000910

Sagawa, H., 2008. Terahertz remote sensing of the Venusian atmosphere: Observations Using the Nobeyama Millimeter Array. Journal of the National Institute of Information and Communications Technology 55, 149–157.

Sandor, B. J., Clancy, R. T., Moriarty-Schieven, G., Mills, F. P., 2010. Sulfur chemistry in the venus mesosphere from {SO2} and {SO} microwave spectra. Icarus 208 (1), 49 – 60.
URL http://www.sciencedirect.com/science/article/pii/S0019103510000874

Steffes, P. G., 1985. Laboratory measurements of the microwave opacity and vapor pressure of sulfuric acid vapor under simulated conditions for the middle atmosphere of venus. Icarus 64 (3), 576 – 585.
URL http://www.sciencedirect.com/science/article/pii/0019103585900776

Steffes, P. G., Eshleman, V. R., 1981. Laboratory measurements of the microwave opacity of sulfur dioxide and other cloud-related gases under simulated conditions for the middle atmosphere of venus. Icarus 48 (2), 180 – 187.
URL http://www.sciencedirect.com/science/article/pii/0019103581901032

Steffes, P. G., Shahan, P., Barisich, G. C., Bellotti, A., 2015. Laboratory measurements of the 3.7–20 cm wavelength opacity of sulfur dioxide and

carbon dioxide under simulated conditions for the deep atmosphere of venus. Icarus 245, 153 – 161.
URL http://www.sciencedirect.com/science/article/pii/S0019103514004746

Student, 1908. The probable error of a mean. Biometrika 6 (1), 1–25.
URL http://biomet.oxfordjournals.org/content/6/1/1.short

Suleiman, S. H., Kolodner, M. A., Steffes, P. G., 1996. Laboratory measurement of the temperature dependence of gaseous sulfur dioxide (so2) microwave absorption with application to the venus atmosphere. Journal of Geophysical Research: Planets 101 (E2), 4623–4635.
URL http://dx.doi.org/10.1029/95JE03728

Tyler, G. L., Howard, H. T., 1969. Refractivity of carbon dioxide under simulated martian conditions. Radio Science 4 (10), 899–904.
URL http://dx.doi.org/10.1029/RS004i010p00899

Waters, J., 1976. 2.3. absorption and emission by atmospheric gases. In: Meeks, M. (Ed.), Astrophysics Radio Telescopes. Vol. 12, Part B of Methods in Experimental Physics. Academic Press, pp. 142 – 176.
URL http://www.sciencedirect.com/science/article/pii/S0076695X08606845

- We measure the millimeter absorption of SO2 in a Venus atmosphere.
- We compare these measurements with previously used formalism.
- We determine which formalism fits better fits the measured data.